The Journal of Experimental Biology 213, 3723-3733

doi:10.1242/jeb.047548

Putative pacemakers of crayfish show clock proteins interlocked with circadian oscillations

Elsa G. Escamilla-Chimal, Rosa María Velázquez-Amado, Tatiana Fiordelisio and María Luisa Fanjul-Moles*

Departamento de Ecología y Recursos Naturales, Facultad de Ciencias UNAM, Avenida Universidad 3000, Ciudad Universitaria, México 04510, México

*Author for correspondence (mfajul@gmail.com)

Accepted 6 August 2010

SUMMARY

Although the molecular mechanisms that control circadian rhythms in many animals, particularly in the fly, are well known, molecular and biochemical studies addressing the location and function of the proteins and genes contributing to the cycling of the clock in crayfish *Procambarus clarkii* are scarce. In this study, we investigated whether three proteins that interact in the feedback loop of the molecular clock described for *Drosophila* are expressed in the putative circadian pacemakers of crayfish retina, eyestalk and brain and whether their expression cycles in a manner consistent with elements of the circadian clock. Here we identified PER, TIM and CLK immunoreactivity in the cytoplasm and nucleus of cells located in the retina as well as in clusters of cells and neuropils of the optic ganglia, lateral protocerebrum and brain. Brain clusters 6, 10, 9 and 11, in particular, showed Per, Tim and Clk-like immunoreactivity at the perikarya and nucleus, and these antigens colocalized at Zeitgeber time (ZT) 0 and/or ZT 12. A biochemical assay demonstrated circadian functionality of Per, Tim and Clk proteins. Both in the eyestalk and in the brain, these proteins demonstrated apparent daily and circadian rhythms. The presence and colocalization of these clock proteins in the cytoplasm and/or nucleus of several cells of retina, optic lobe and brain, depending on time, as well as their circadian oscillations, suggest interactions between positive and negative transcription factors and clock proteins similar to those forming the feedback loop of the canonical model proposed for different animals.

Key words: circadian clock, protein, pacemaker, crayfish.

INTRODUCTION

Circadian clocks enable organisms to anticipate predictable environmental changes, schedule activities for an advantageous time of the day, and coordinate internal processes with the environment. The molecular control of circadian rhythms in animals is best known in the fruit fly, *Drosophila melanogaster*, and involves interactions among the transcription factors Period (dPER), Timeless (dTIM), Clock (dCLK), Cycle (dCYC), Par Domain Protein 1, Vrille; the kinases Double-Time, Shaggy and Casein Kinase 2; as well as Protein phosphatase 2a and the protein degradation protein Supernumerary limbs (Hardin, 2005; Hardin, 2009). The proteins dCLK and dCYC interact and form a complex that binds E-box elements (CACGTG) in regulatory sequences of the *Per* and *Tim* promoter regions to activate their transcription. The mRNA transcripts of these genes accumulate in the cytoplasm of pacemaker cells, where they are translated into proteins. The protein products dPER and dTIM accumulate at night, entering the nucleus and binding to the CLK–CYC complex. The binding of dPER and/or dTIM to the CLK–CYC complex interferes with the binding of the complex to the E-box and results in a cessation of transcriptional activity (Darlington et al., 1998). By this feedback loop, dPER and dTIM inhibit their own transcription. Degradation of dTIM late at night renders dPER unstable and leads to its degradation later in the morning. These events release the inhibition from CLK–CYC and enable a new cycle of *Per*, *Tim*, *Vri* and *dPdp* transcription. The negative feedback loop is tuned by the action of cryptochrome (dCRY), the kinases and the phosphatases (for a review, see Hardin, 2005; Dubruille and Emery, 2008). dCRY allows the synchronization of the clock. The CLK–CYC complex is involved in a second autoregulatory loop in the fly pacemaker that controls the cycling levels of dCLK. A comparison of the mechanisms for rhythm generation between vertebrates and flies reveals that there is a high degree of conservation in the design and function of the clock and that similar clock genes are involved in these two models, although some of these genes appear to take on different functions in the clocks of the fly and the mouse (Stanewsky, 2003).

The crayfish is an interesting model for proteomics and molecular analysis of circadian rhythms because its clock system has been implicated in a set of complex behaviors, such as foraging, social and maternal behavior and, sometimes, migration (De Coursey, 1983). Although there has not been a formal study relating the clock to these behaviors in crayfish, a variety of overt circadian rhythms controlled by periodic function of the nervous system has been studied (Fanjul-Moles and Prieto-Sagredo, 2003; Fanjul-Moles, 2006) and different experiments have identified several neuronal tissues containing separate circadian clocks that form complex interactions. These exist within the brain (supraesophageal ganglion) (Page and Larimer, 1975a; Page and Larimer, 1975b; Larimer and Smith, 1980; Barrera and Block, 1990; Sullivan et al., 2009), the retina of the eye (Aréchiga and Rodriguez-Sosa, 1998) and the eyestalk (Aréchiga and Rodríguez-Sosa, 2002). Many experiments that have focused on neural and endocrine aspects suggest that the circadian system of crayfish is a distributed circadian clock system. However, molecular and biochemical studies addressing the location and function of the proteins and genes contributing to the cycling of the clock are scarce (Aréchiga and Rodriguez-Sosa, 1998; Fanjul-Moles et al., 2004; Yang et al., 2006; Escamilla-Chimal and Fanjul-Moles, 2008).

In the present study, we contribute to this knowledge by investigating whether three proteins that interact in the feedback loop of the molecular clock described for *Drosophila*, PER, TIM and CLK, are expressed in the putative circadian pacemakers of crayfish retina, eyestalk and brain and whether they cycle in a manner consistent with elements of the circadian clock.

MATERIALS AND METHODS

Animals and experimental design

We used *Procambarus clarkii* (Girard 1852) of homogenous size and mass (mean ± s.e.m.; 11±1 cm from rostrum to telson and 29.6±1.2 g) in the intermolt stage. A total of 180 male adults were field-collected from Delicias, Chihuahua in northern Mexico at latitude of 28°N. Their sibling relationship was unknown. Crayfish were acclimatized to the laboratory for one month in aquaria placed under natural light:dark (L:D) cycle conditions at 20°C, pH 7.9 and 5.7 mg l^{-1} O_2. All the animals were fed *ad libitum* with a vegetable diet. The aquaria contained polyvinyl tubes simulating burrows, which allowed the animals to hide from light. After acclimatization, the animals were divided into two batches, one for biochemical analysis and the other for histological analysis. The first batch consisted of one group of 54 animals subjected to 12 h:12 h L:D cycles for 15 days, and another two groups of 54 animals each that were treated as described (12 h:12 h L:D) and subsequently exposed to continuous darkness (D:D) for 24 or 72 h. At the end of each treatment, nine specimens from each group were selected at random at six different times of day, anesthetized on ice and killed before processing for western blotting (Table 1).

The second batch consisted of one group of 18 animals subjected to a 12 h:12 h L:D cycle for 15 days, at the end of which nine specimens were selected at random at two time points: lights-on time [07.00 h, Zeitberger time (ZT 0)] and lights-off time (19.00 h, ZT 12). (NB. Zeitberger time is a standardized 24 h notation of the phase in an entrained circadian cycle, where ZT 0 indicates the onset of day, or the light phase, and ZT 12 indicates the onset of night, or the dark phase.) Specimens were anesthetized on ice and killed before processing for histological analysis (Table 1).

At each experimental time point, the eyestalk–supraesophageal ganglion complex of each animal was dissected and processed for histological or biochemical analysis. We explored the following time points: 07.00 and 19.00 h in organisms processed for histology and 07.00, 11.00, 15.00, 19.00, 23.00 and 03.00 h in organisms analyzed by biochemical techniques.

Histological procedures

Crayfish were anesthetized with ice for 15 min before decapitation. The whole eyestalk–brain complex was dissected and fixed in Bouin's fixative at 4°C for 12 h, after which the tissues were rinsed three times, for 30 min each, in phosphate-buffered saline (PBS). Fixed tissues were embedded in 3.0% low-melting-point agarose (Invitrogen, Carlsbad, CA, USA) dissolved in 0.1 mol l^{-1} PBS. The agar block was glued with cyanoacrylate onto the plate of a Vibratome (Series 3000 plus; Vibratome, St Louis, MO, USA). The slicing chamber was then filled with PBS and 200 µm-thick sagittal slices were prepared using a vibrating blade microtome. Slices were incubated in blocking solution containing 2% bovine serum albumin (BSA) (w/v; BSA fraction V; Gibco-BRL, Rockville, MD, USA), 1% horse serum and 1% Triton X-100 (v/v; Gibco-BRL) at 4°C for 48 h. We used the following commercially available antiserums: *Drosophila* anti-PER generated in chicken (Alpha Diagnostic International, San Antonio, TX, USA), anti-mouse TIM generated in rabbit (Santa Cruz Biotechnology, Santa Cruz, CA, USA) and *Drosophila* anti-CLK generated in goat (Santa Cruz Biotechnology).

Table 1. Experimental treatment and subsequent analysis of batches of *P. clarkii*

Treatment	*N*	Analysis
12 h:12 h L:D	18	Histology
12 h:12 h L:D	54	Western blotting
12 h:12 h L:D + 24 h D:D	54	Western blotting
12 h:12 h L:D + 72 h D:D	54	Western blotting

N, number of crayfish; L:D, light:dark cycle; D:D, continuous darkness.

Samples were incubated overnight at 4°C with the primary anti-PER, anti-CLOCK or anti-TIM polyclonal antibody diluted in blocking solution (1:50, 1:100 and 1:100, respectively) with 0.1% Triton X-100 in a humid chamber. Samples were then washed and incubated for 2 h at room temperature with the respective secondary antibody (1:100 dilution; Invitrogen): Alexa-Fluor-488-conjugated anti-chicken (for PER), Alexa-Fluor-543-conjugated anti-rabbit (for TIM) and Alexa-Fluor-647-conjugated anti-goat (for CLOCK). After several washes with PBS for 3 min each, samples were incubated for 5 min with 4′,6-diamidino-2-phenylindole, dilactate (DAPI dilactate) (Invitrogen) washed and mounted with medium containing 15 mmol l^{-1} NaN_3 (DAKO, Carpinteria, CA, USA). Negative controls were prepared by reacting samples with either the primary or the secondary antibody. All controls were pre-adsorbed with the corresponding control peptide.

Some organs were incubated with paraplast after fixation in Bouin's fixative and cut into longitudinal sections (20 µm thick) using a microtome (Leitz 1512; Ramsey, MN, USA). The slides were incubated with the same primary polyclonal antibodies as mentioned above: *Drosophila* anti-PER generated in chicken (Alpha Diagnostic International), diluted 1:100 (v/v) in PBS, and anti-mouse TIM generated in rabbit (Santa Cruz Biotechnology), diluted 1:100 (v/v) in PBS, at 4°C for 16 h. The tissues were then incubated with secondary antibodies, Alexa-Fluor-488-conjugated anti-chicken and Texas Red-conjugated anti-rabbit, respectively, and the samples were then incubated with DAPI (1:1000; Invitrogen) for 5 min.

Image analysis and microscopy

Mounted slices were viewed by epifluorescence microscopy using a DMI 6000 inverted microscope (Leica Microsystems, Wetzlar, Germany) equipped with a Leica EL6000 external EL6000 mercury light source for enhanced fluorescence imaging connected *via* a liquid light guide and a filter set appropriate for Alexa Fluor 488 [excitation band pass (BP) 480/40 nm, dichromatic mirror 505 nm and emission filter BP 527/30], Alexa Fluor 543 (BP 546/12 nm, 565 nm and BP 600/40), Alexa Fluor 647 (BP 620/60 nm, 660 nm and BP 700/75) and DAPI [BP 340/380 nm, 400 nm and long pass (LP) 425]. For total tissue reconstruction, samples were examined with a 20× Plan APO objective (multiple immersion 0.7 NA; Leica Microsystems) and some images were taken with high magnification using 40× or 60× Plan APO objectives (oil immersion 1.25 NA; Leica Microsystems). Digital images were acquired with a cooled CCD digital camera (DFC345 FX; Leica Microsystems). Exposures were chosen for the range of fluorescence intensities of each primary antibody. Images were acquired with Leica AF software and stored in Lif or TIFF image format (8 or 12 bits resolution).

Some mounted slices (20 µm) were visualized by means of Apotome AX10 Imager.Z1 microscopy (Zeiss, Jena, Germany), with a filter for Alexa Fluor 488 (excitation BP 493 nm, emission filter BP 520), Texas Red (510–560 nm, 590) and DAPI (358 nm, 463).

Biochemical determination

Protein sample preparation

Brain–eyestalk complexes, including the retina, were carefully homogenized in 100 µl of ice-cold PBS, pH 7.4. The homogenates were then centrifuged at 11,000 ***g*** for 25 s at room temperature. Supernatants were stored at −71°C until analyzed. Samples were thawed at room temperature, and the protein concentration was determined using the Bradford assay (Bradford, 1976) and standards of 3.75, 11.25, 18.75, 26.25 and 37.5 µg µl^{-1} BSA (Sigma-Aldrich, St Louis, MO, USA).

Western blotting

Proteins were separated using denaturing sodium dodecyl sulfate polyacrylamide gel electrophoresis (SDS-PAGE) (Laemmli, 1970) with a 10% polyacrylamide separating gel. Each lane was loaded with 40 µg of protein, except for the positive control (control peptide; Alpha Diagnostic International, Inc. or Santa Cruz Biotechnology) and the molecular mass standards.

Proteins resolved by SDS-PAGE were electrophoretically transferred from the gels to polyvinylidene fluoride (PVDF) Immobilon transfer membranes (Millipore, Billerica, MA, USA) by routine methods using a Mini Trans-Blot system (Bio-Rad, Hercules, CA, USA) at 100 V for 45 min. Protein loading efficacy and localization for molecular mass determination were revealed by staining with Coomassie Blue. The blots were incubated for 16 h at room temperature with the previously described *Drosophila* anti-PER, anti-CLK and mouse anti-TIM antiserums diluted 1:500, 1:1000 and 1:1000 (v/v), respectively, in 1% gelatin solution. Blots were then rinsed with Tris buffer saline (TBS) then twice with TTBS (350 µl Tween-20 diluited in 700 ml TBS), and incubated with peroxidase anti-chicken (1:4000; Jackson ImmunoResearch Laboratories, Biosetec, West Grove, PA, USA) anti-rabbit (1:30,000; Alpha Diagnostic International) and anti-goat (1:30,000; Abcam, Cambridge, MA, USA) antibodies for 2 h at room temperature. The membranes were subsequently processed for chemiluminescent detection using Super Signal West Pico Chemiluminescent substrate (Thermo Fisher Scientific, Rockford, IL, USA). The specificity of each antibody was determined by blocking with a peptide control at 4°C for 24 h; afterwards, the antibody was used for western blotting. Rabbit anti-GAPDH antiserum (1:1000; Abcam) was used as a loading control. The blots were scanned and digitized with the Gel Logic 200 Imaging System (Eastman Kodak, Rochester, NY, USA). Bands were quantified in a computerized analyzer system using the Kodak Molecular Imaging software version 4.4. For each experiment, the data (mean intensity of the immunoreactive area of the band) obtained for each time point were averaged and expressed as the means ± s.e.m. of PER, TIM or CLK relative abundance, normalized to the GAPDH values.

Data analysis

Chronograms were constructed using the group mean ± s.e.m. To estimate circadian rhythms for each biochemical parameter (PER, TIM and CLK) for the different experimental groups, a single cosinor analysis was performed using COSANA software (Menna-Barreto et al., 1993). Based on a test period(s), cosinor analysis adjusts data to a cosine function and provides an objective test of whether the rhythm amplitude differs from zero (Nelson et al., 1979). This method provides descriptive estimators for a number of different rhythm parameters, including acrophase, mesor, amplitude and percentage of rhythmicity (PR). Acrophase represents the crest time of the best-fitting mathematical function approximating the data, expressed as an interval from a designated phase reference, in this case the local midnight (00.00 h), whereas mesor comprises the value around which oscillation occurs; when the time interval between data samplings is constant, it equals the arithmetic mean of the rhythmic oscillation. In the present study, it corresponds to the arithmetic mean of the rhythmic oscillation of the expression of PER, TIM or CLK over a 24 h period. The amplitude is equal to one-half of the difference between the highest and lowest oscillation values, and PR is the percentage of data included within the 95% confidence limits of the best-fitting cosine function. This test allows objective examination of the hypothesis that amplitude of the temporal oscillation differs from zero using different trial-period lengths. In the present study, several periods were tested to analyze whether temporal biochemical profiles under the different L:D

Table 2. Single cosinor analysis of PER, TIM and CLK abundance (% area) in *P. clarkii* eyestalk and brain

	Treatment	Period (h)	Mesor	Amplitude	Acrophase	PR (%)	*P*
PER							
Eyestalk	12 h:12 h L:D	24	55.47	12.65	13.19	8.84	0.054
	24 h D:D	27.36	54.26	18.77	16.09	17.61	**0.001**
	72 h D:D	22	45.37	18.8	15.36	16.91	**0.002**
Brain	12 h:12 h L:D	24	49.99	17.85	1.14	19.28	**0.004**
	24 h D:D	24	55.3	16.41	12.45	10.76	**0.022**
	72 h D:D	23	48.17	20.46	9.50	18.68	**0.008**
TIM							
Eyestalk	12 h:12 h L:D	22.23	50.02	15.71	2.52	10.15	**0.007**
	24 h D:D	12.11	69.52	21.27	3.20	28.02	**0.001**
	72 h D:D	25.23	52.06	22.56	5.45	22.36	**0.004**
Brain	12 h:12 h L:D	24	56.07	11.66	22.19	7.48	0.181
	24 h D:D	21.36	44.20	20.79	17.32	18.86	**0.017**
	72 h D:D	23.00	65.55	18.66	4.33	21.22	**0.010**
CLK							
Eyestalk	12 h:12 h L:D	24	25.5	35.48	18.47	53.89	**0.000**
	24 h D:D	24	65.26	16.3	11.05	15.97	**0.012**
	72 h D:D	23.23	58.61	11.19	8.33	7.79	**0.050**
Brain	12 h:12 h L:D	24	69.54	14.03	21.45	16.71	**0.028**
	24 h D:D	12	72.71	12.16	5.49	14.42	**0.005**
	72 h D:D	24	62.08	35.86	7.42	71.47	**0.000**

Mesor, arithmetical mean of the adjusted rhythm; PR, percentage of rhythmicity; L:D, light:dark cycle; D:D, continuous darkness. Significant results (P<0.05) are shown in bold.

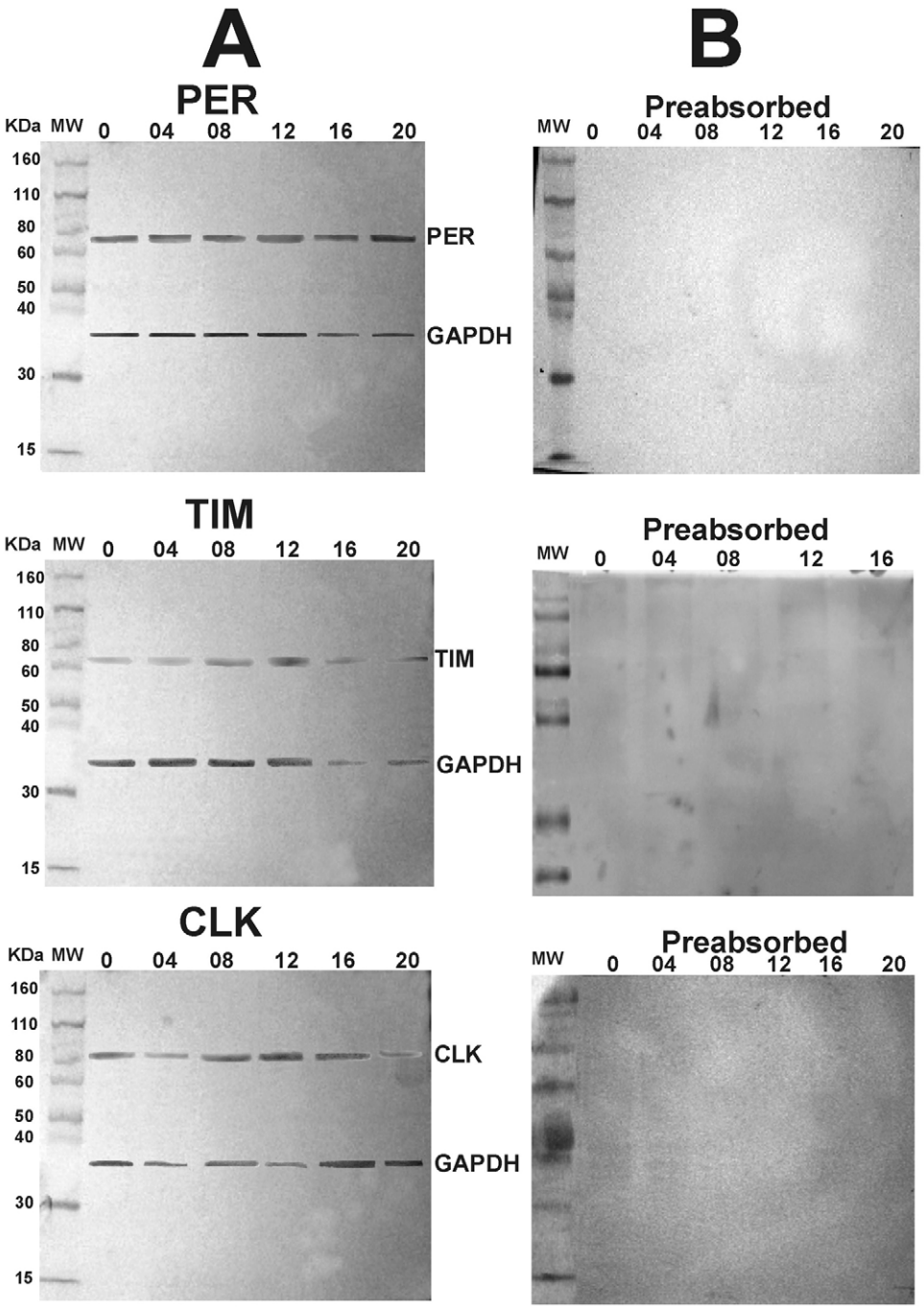

Fig. 1. (A) Representative western blot analysis showing the positivity of PER, TIM and CLK antibodies to *P. clarkii* brain at six different time points of a 12 h:12 h L:D cycle. (B) After incubation of the antibodies with the corresponding control peptides (see Materials and methods), the immunoreactive bands are not present, indicating the specificity of the antibodies. Each lane represents a time point of sample collection from animals maintained in L:D conditions. The left side of the figure shows the position of molecular mass markers. Loading control is shown by GAPDH.

conditions are indeed circadian. Values are expressed as means ± s.e.m., and $P<0.05$ was considered significant for rhythm detection, i.e. non-zero amplitude.

RESULTS

Biochemical validation of antibody specificity

Analysis of the extracts of crayfish eyestalks and brain revealed the presence of proteins that are immunoreactive to anti-PER, anti-TIM and anti-CLK antibodies. The polyclonal antibodies used in this study recognized PER, TIM and CLK in the retina, eyestalk and brains as bands migrating with an apparent molecular mass of approximately 70, 60 and 80 kDa, respectively (Fig. 1). The molecular mass of the bands is consistent with the molecular mass of the amino acid sequences reported for *Drosophila simulans* PER (UniProt Q03355), *Ratus norvergicus* TIM (UniProt B1WBQ6) and *Macrobrachium rosenberg*i CLK (GenBank AAX4405).

Immunohistochemistry

ZT 0

Eyestalk

At ZT 0, we detected PER immunoreactivity (PER-ir) and TIM-ir in the photoreceptors and tapetal cells of the retina, respectively. PER-ir was located in the lamina ganglionaris (LG) in the synaptic or cartridge region and in the proximal glial sheath (PGS) (Hafner, 1973; Nassel, 1977) (Fig. 2A,B). Immunohistochemistry [Fig. 2A,B, as well as merged images (data not shown)] revealed the presence and colocalization of PER-ir and TIM-ir in the optic neuropils, particularly in the external medulla (EM) and terminal medulla (TM).

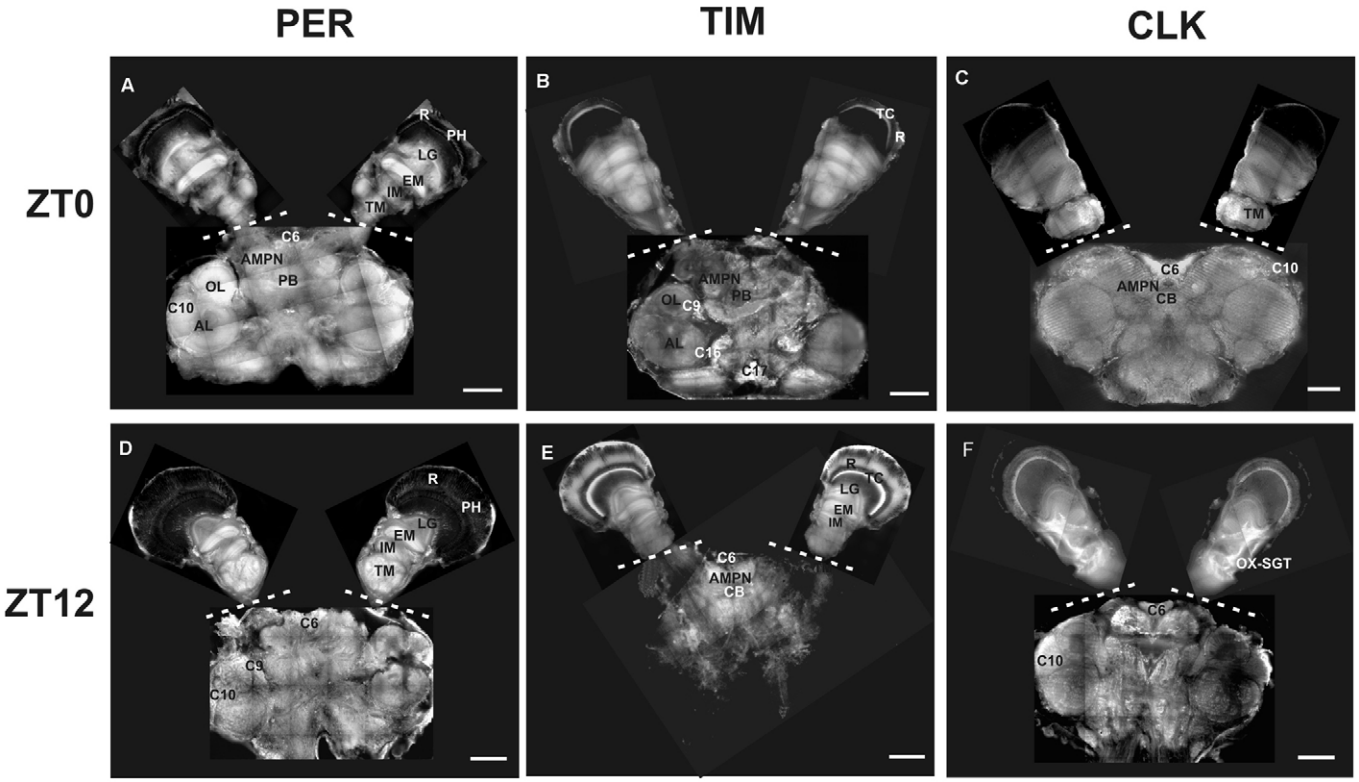

Fig. 2. PER, TIM and CLK immunoreactivity in the brain and eyestalk ganglia of *P. clarkii* at ZT 0 (A–C) and ZT 12 (D–F). (A) PER-ir is expressed in the retina in the photoreceptor area and lamina, in perikarya in cell clusters throughout the eyestalk optic ganglia and in the brain in clusters 6 and 10, in the anterior median protocerebral neuropil (AMPN) and the central body (CB). (B) TIM-ir is expressed in the retina (R) in the tapetal cells (TC) and throughout the eyestalk ganglia and the brain, in clusters 9, 16 and 17. (C) CLK-ir appears in the eyestalk in the lateral brain in the terminal medulla (TM) and in the medial brain in the AMPN and the CB. The olfactory and accessory lobes (OL and AL), as well as clusters 6 and 10, show CLK-ir. (D) PER-ir is expressed in the photoreceptors and throughout the eyestalk, in cells and neuropils of optic ganglia, and throughout the brain in somata of clusters 6, 9 and 10. (E) TIM-ir is shown in the retina and lamina, as well as in the external and internal medullas (EM and IM) in the brain. TIM-ir is shown in the AMPN and in some cells of cluster 6 and the CB. (F) CLK-ir is expressed in the retina and the eyestalk in the brain at clusters 6 and 10 and the median neuropils. Scale bars: 500 μm. C, cell cluster; LG, lamina ganglionaris; PB, protocerebral bridge; PH, photoreceptors; XO-SGT, X-organ sinus gland tract.

Conversely, at this time of day, all of the structures of the eyestalk showed a dim and diffuse CLK-like immunoreactivity, which was only clear at the TM (Fig. 2C). Double-labeling experiments verified PER and TIM colocalization in various immunoreactive somata and projections in the retina and lamina. Fig. 3A shows intense PER-ir in the synaptic region at the cartridges and in the inner ganglion cell layer (IGL), where the cytoplasm and nucleus of some perikarya show PER-ir and TIM-ir. Below the synaptic region, some small cells in the PGS also showed PER-like immunofluorescence (Fig. 3A). Some cells that showed strong PER-ir were located lateral to the EM, with a group of cells falling between the optic lobe medullas and the hemiellipsoid body (HB) (see Fig. 3B–D).

Fig. 4A,B shows TIM-ir and CLK-ir in the eyestalk neuropils, as well as in a group of cells located in the EM, internal medulla (IM) and in the anterior region of the TM, where strong TIM–CLK colocalization was evident (Fig. 4C). By contrast, Fig. 4B revealed CLK-ir in the perikarya and nucleus of a group of cells located between the EM and IM, as is shown in Fig. 4C (arrow).

Brain

PER- and TIM-like immunoreactivity (Fig. 2A,B) were detected in the brain at the median protocerebrum. PER-ir was present in some cells of clusters 6 and 10, as well as in the anterior median protocerebral neuropil (AMPN) and the protocerebral bridge (PB). Meanwhile, CLK-ir was observed in the cells of clusters 6 and 10 and the central body (CB) (Fig. 2C). The signal was particularly strong in cluster 6. At this time of day, PER-, TIM- and CLK-ir were also detected in the olfactory and accessory lobe (OL and AL) neuropils (Fig. 2A–C). Some cells of clusters 9, 16 and 17 showed TIM-ir but did not show PER- or CLK-ir (Fig. 2A–C). Details of the immunoreactivity of these antigens in the brain may be observed in Fig. 3E, which reveals PER-ir in cluster 10, and in Fig. 4D, which shows TIM-ir in clusters 6 and 10, the OL, the AL and the PB. By contrast, Fig. 4E shows CLK-ir in clusters 6 and 10 and the above-mentioned neuropils. This antigen signal was particularly strong at cluster 6. A merged image (Fig. 4F) reveals TIM and CLK in the AMPN, the CB, and the OL and AL neuropils.

ZT 12

Eyestalk

Although the difference was not quantified, at ZT 12 we detected increased levels of PER-ir and TIM-ir in the retina and lamina compared with ZT 0. In the retina (Fig. 2D,E), at this time of day, immunofluorescence revealed the presence of CLK-ir in the retinular and tapetal cells (Fig. 2F). Details of the immunoreactivity of these antigens may be observed in Figs 5 and 6. PER-ir was detected in the photoreceptor zone (Fig. 5A), where axons penetrated the basement membrane, going towards the plexiform

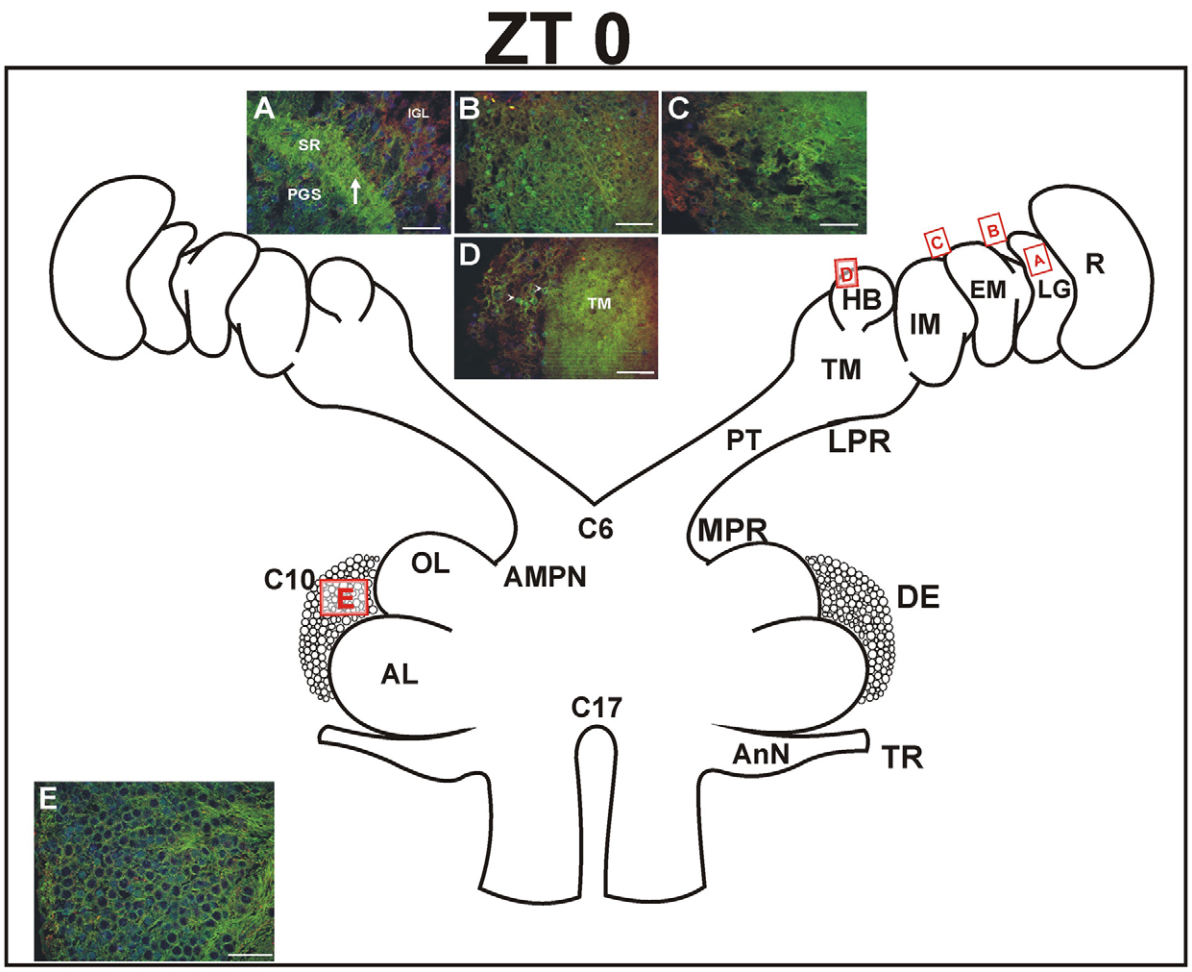

Fig. 3. Representative Apotome images of double-immunostained structures of *P. clarkii* eyestalk and brain at ZT 0. PER (green), TIM (red), DAPI (blue). (A) PER-ir is located in the lamina ganglionaris (LG) mainly in the cartridge region (arrow), the synaptic region and the proximal glial sheath (PGS). TIM is located in some cells of the inner ganglion cell layer (IGL). (B) PER (green) is shown in the perikarya and nucleus of cells located between the LG and the external medulla (EM). (C) A group of cells located between the EM and the internal medulla (IM) show TIM (red) and PER (green). (D) Arrowheads show PER-ir (green) in the perikarya and nucleus of some cells located in the lateral region of the terminal medulla (TM). (E) Cluster 10 (C10) of the deutocerebrum (DE). Scale bars: 40 μm. AL, accessory lobe; AMPN, anterior median protocerebral neuropil; AnN, antennal neuropil; C, cell cluster; HB, hemiellipsoid body; LPR, lateral protocerebrum; MPR, medial protocerebrum; OL, olfactory lobe; PT, protocerebral tract; R, retina; TM, terminal medulla; TR, triticerebrum.

layer in the lamina. Fig. 5B,C shows CLK-ir in the retinular and tapetal cells. Fig. 6 shows PER (Fig. 6A) and TIM (Fig. 6B) colocalizing in the proximal lamina (Fig. 6C), where the cartridge region is located. At this time of day, TIM-ir was present in the tapetal cells. In the LG, this antigen was mainly localized to the plexiform layer (Fig. 6B).

The optic lobes had TIM-ir in the EM and IM as well as CLK-ir in the IM, whereas PER-ir was seen in all optic ganglia (Fig. 2D–F). Interestingly, a group of axons linking the EM to the lateral protocerebrum, which was probably the X-organ sinus gland tract (XO-SGT), showed CLK-ir (Fig. 2F). Details of the localization of the three antigens can be seen in Fig. 5D and Fig. 6D. PER-ir was detected in a group of cells located between the EM and IM (Fig. 5D). These cells might correspond to those expressing red pigment concentrating hormone (RPCH), described previously for crayfish (Preciado et al., 1994).

Brain

In the brain, a small group of protocerebral cells in cluster 6 and some cells in clusters 10 and 9, as well as the OL and AL, showed PER-ir (Fig. 2D). However, only the AMPN, a group of cells of cluster 6 and the CB (Fig. 2E) showed TIM-ir.

Moreover, although this was not quantified, the brain showed stronger CLK immunolabeling at ZT 12 than at ZT 0. This antigen was detected in the AMPN, in a group of cells in protocerebral cluster 6, in some perikarya in the deutocerebrum at cluster 10 and in the CB in the median protocerebrum (Fig. 2F). Fig. 5E,F demonstrates the presence of PER-ir and TIM-ir in the perikarya of some cells of cluster 6. One of these large neurons (60 μm diameter) showed PER in the nucleus. Fig. 5G reveals colocalization of both antigens.

Biochemical analysis

Chronograms showing the temporal changes in the relative abundance of the clock proteins in the eyestalk and brain are depicted in Figs 7 and 8. Eyestalk TIM and CLK showed significant daily oscillations in abundance under L:D conditions ($P<0.01$, $P<0.01$), with peak levels of TIM and CLK occurring at night from ZT 16.00 to 20.00 and ZT 12.00, respectively. Unexpectedly, the peak of PER occurred during the day at ZT 04.00 h. Under 24 and 72 h D:D, the

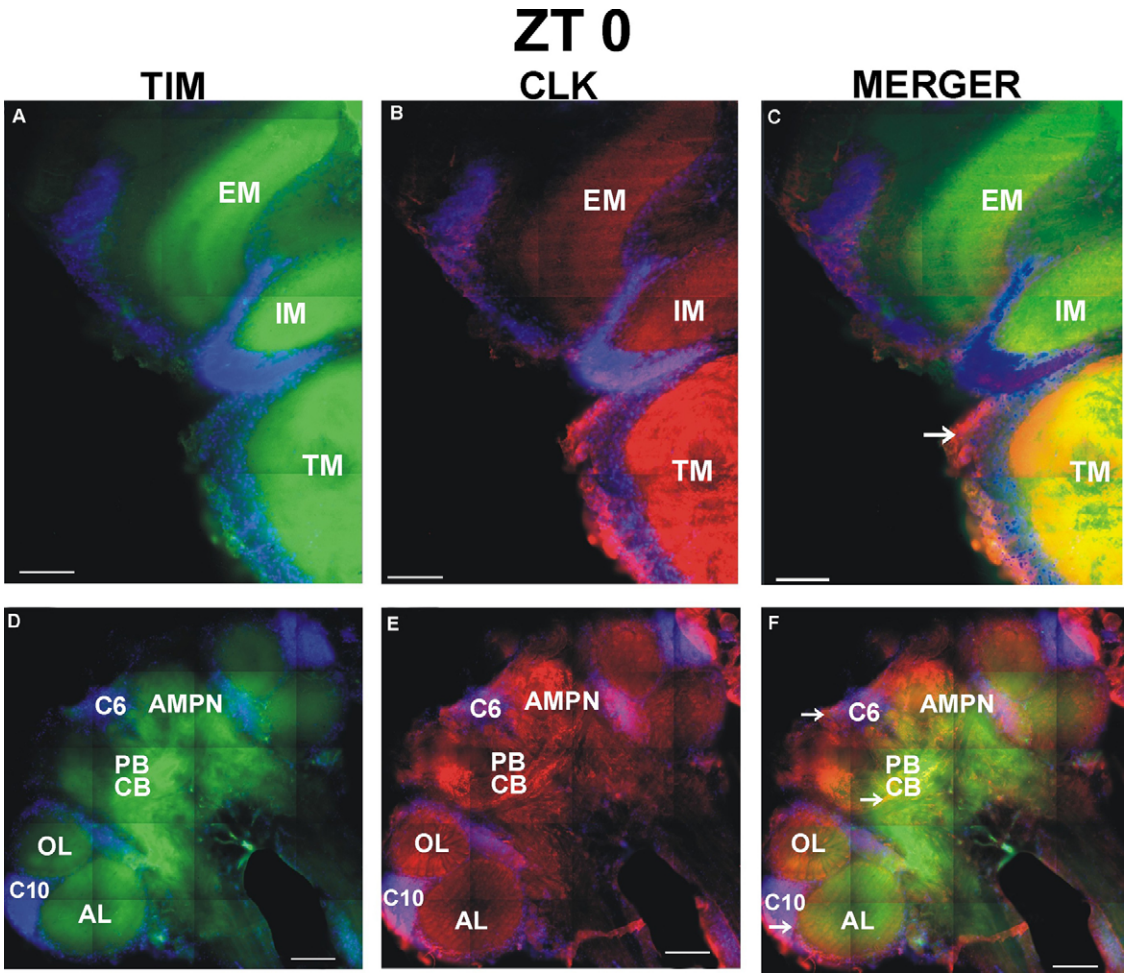

Fig. 4. Distribution of TIM and CLK immunofluorescence in the optic ganglia and brain of *P. clarkii* at ZT 0. (A) TIM-ir (green), (B) CLK-ir (red), DAPI (blue) and (C) merger of three images. Both antigens seem to colocalize in the terminal medulla (TM; yellow). (D) TIM-ir in brain, (E) CLK-ir in brain and (F) merger revealing colocalization of both antigens in the brain. TIM and CLK colocalize in the protocerebral bridge (PB) (see arrow), and CLK-ir may be seen in cells of cluster 6 (C6) and in the PB. The olfactory and accessory lobes (OL and AL) show TIM-ir and CLK-ir in cluster 10 (C10). Arrows show CLK-ir colabeling with DAPI, indicating the presence of CLK-ir in the nucleus of some of these cells. In PB and CB, arrow shows TIM colabeling with CLK (yellow fringe). Scale bars: 100 μm (A–C) and 300 μm (D–F). EM, external medulla; IM, internal medulla.

oscillations in PER abundance persisted and showed increased statistical significance (P<0.001, N=9) (Table 2), cycling with a bimodal oscillation with two troughs corresponding to the onset and offset of light (Fig. 7B) after 24 h DD. There was a statistically significant circadian rhythm after 72 h D:D (τ=22 h, P<0.001, N=9), with a maximal peak at 03.00 h that is a mirror image of the previous 24 h daily rhythm that appeared in L:D (Table 2). The daily oscillation in TIM abundance after 24 h D:D shows a markedly bimodal, statistically significant oscillation, and a clear circadian oscillation appears after 72 h D:D (Table 2). In D:D, the oscillation in CLK abundance persisted after both 24 and 72 h (P<0.01 and P<0.05, respectively, N=9), doubling the cycle activity level (Table 2) and showing circadian period (τ) values (τ=24 h and τ=23.2 h, respectively), with peak levels occurring at 15.00 and 07.00 h, respectively.

Temporal changes in PER, TIM and CLK abundance in the crayfish brain are shown as chronograms in Fig. 8.

Indeed, cosinor analysis reveals that the relative abundance of PER and CLK underwent statistically significant daily and circadian oscillations in the brain (PER P<0.05, N=9, P<0.01, N=9 and CLK P<0.05, N=9, P<0.01, N=9, respectively). As expected, the PER and TIM cycles peaked at night at ZT 20.00 and from ZT 16.00 to ZT 20.00 h, respectively, whereas CLK peaked at the beginning of the night at 16.00 h. After 24 and 72 h D:D, the daily robust oscillations of the abundance of the three proteins persisted without changes in the oscillation levels (see Table 2), although there were changes in phase and period values. The period of PER and TIM cycles shortened after 72 h D:D, increasing in amplitude and depicting a phase angle of 4 h. PER peaked at night at 03.00 h, and TIM peaked at 23.00 h (external time). The oscillation amplitude of CLK increased markedly after 72 h, showing a period of 24 h and a peak during the day at 07.00 h.

DISCUSSION

The objective of the present study was to understand the cellular basis of the circadian clock of crayfish. Here we show PER-, TIM- and CLK-ir in the cytoplasm and nucleus of specific sets of crayfish neurons located in the retina, optic lobe and brain. Similar data on the presence of PER-ir in the retina and lamina have been previously reported for *Procambarus clarkii* (Aréchiga and Rodríguez-Sosa, 1998), but the presence of PER, TIM and CLK in the eyestalk and brain and their changes in abundance at two different times of day

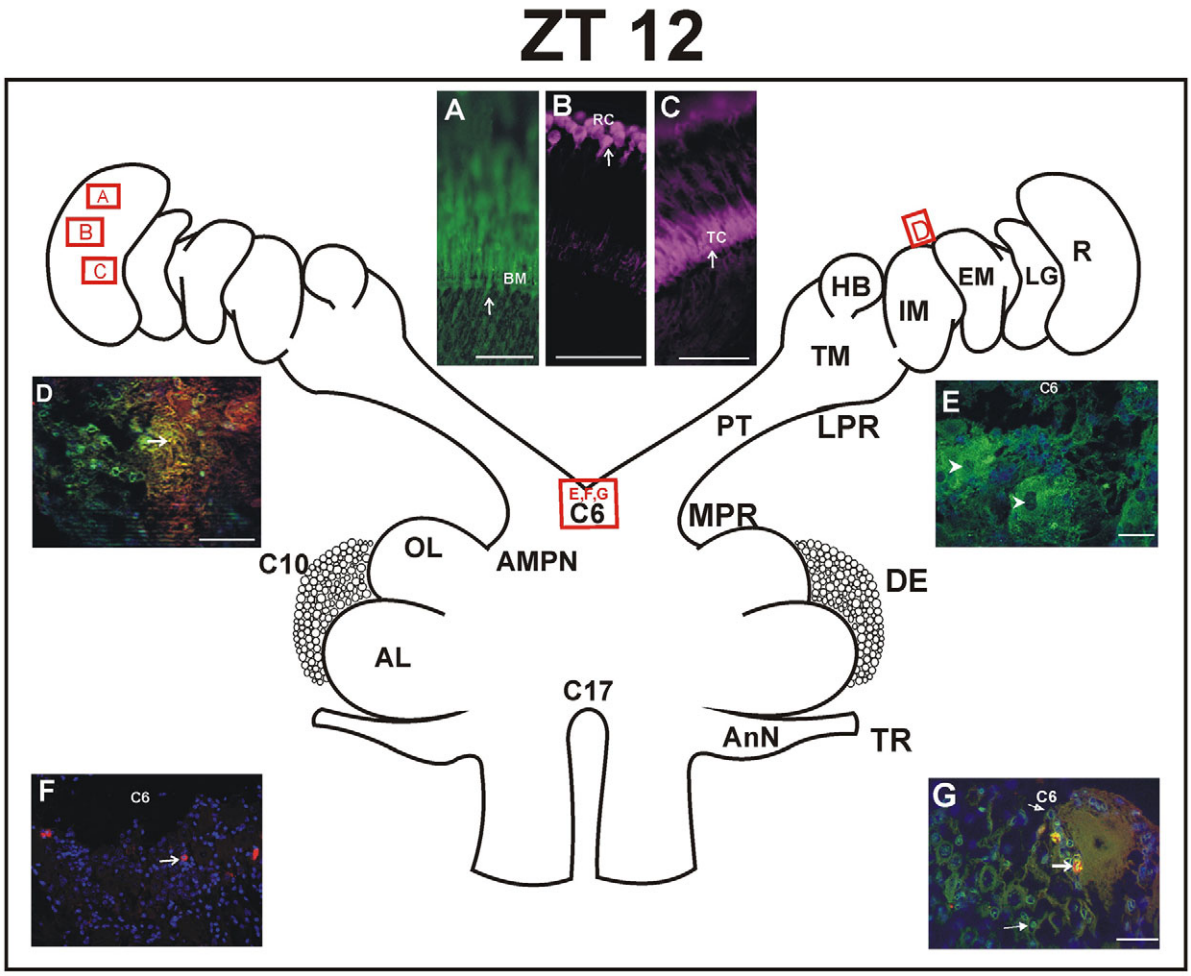

Fig. 5. Immunostaining with anti-PER, anti-TIM and anti-CLK antibodies in various cell types in the retina optic lobe medullas and brain of *P. clarkii* at ZT 12. (A) PER-ir (green) is shown in the photoreceptor area and basal membrane (BM) (arrow). (B) CLK positivity (violet) in the retinular cells (RC), apparently in the nucleus (arrow). (C) CLK-ir in tapetal cells (TC) (arrow). Scale bars: 100 μm. Apotome microscope images showing PER (green) and TIM (red) immunoreactivity with DAPI (blue) in some structures of the eyestalk and brain at ZT 12. (D) PER (green) and TIM (red) colocalize in some groups of cells between the external and internal medullas (EM and IM; yellow). (E) Cells of cluster 6 (C6) showing perikarya and nucleus PER ir (arrowheads). (F) Cells of C6 showing TIM-ir in cytoplasm (arrow). (G) Cells of C6 showing PER (green) and TIM (red) immunoreactivity. Note colocalization of both antigens in yellow (thick arrow). PER-ir is shown both in the nucleus (thin arrow) and cytoplasm (open arrow). Scale bars: 40 μm. AL, accessory lobe; AMPN, anterior median protocerebral neuropil; AnN, antennal neuropil; C, cell cluster; DE, deutocerebrum; HB, hemiellipsoid body; LG, lamina ganglionaris; LPR, lateral protocerebrum; MPR, medial protocerebrum; OL, olfactory lobe; PT, protocerebral tract; R, retina; TM, terminal medulla; TR, tritocerebrum.

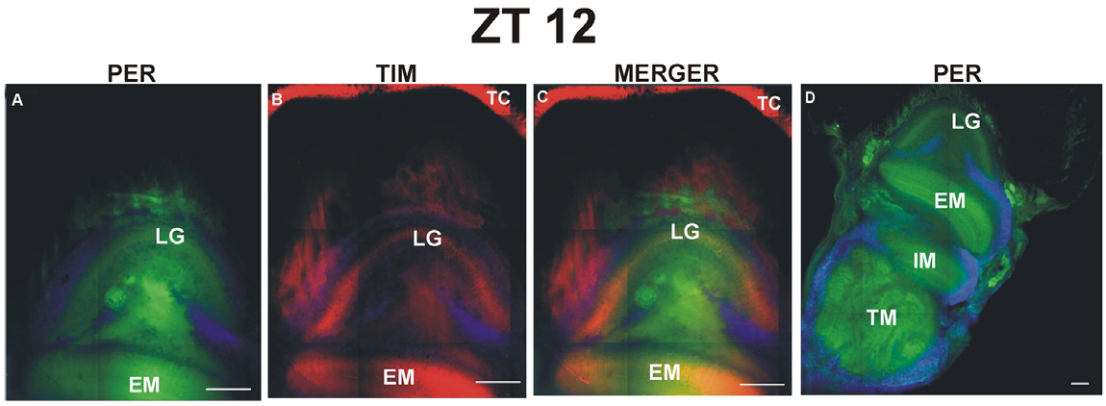

Fig. 6. Distribution pattern of TIM and PER immunofluorescence in the eyestalk of *P. clarkii* at ZT 12. (A) PER (green) and (B) TIM (red) immunopositivity with DAPI (blue) in retina tapetal cells (TC) and (C) merger showing that both antigens colocalize mainly in the lamina ganglionaris (LG) and in the external medulla (EM) neuropil (yellow). (D) PER-ir in all of the medulla neuropils [EM, internal (IM) and terminal (TM)], as well as in groups of cells located among them. Scale bars: 100 μm.

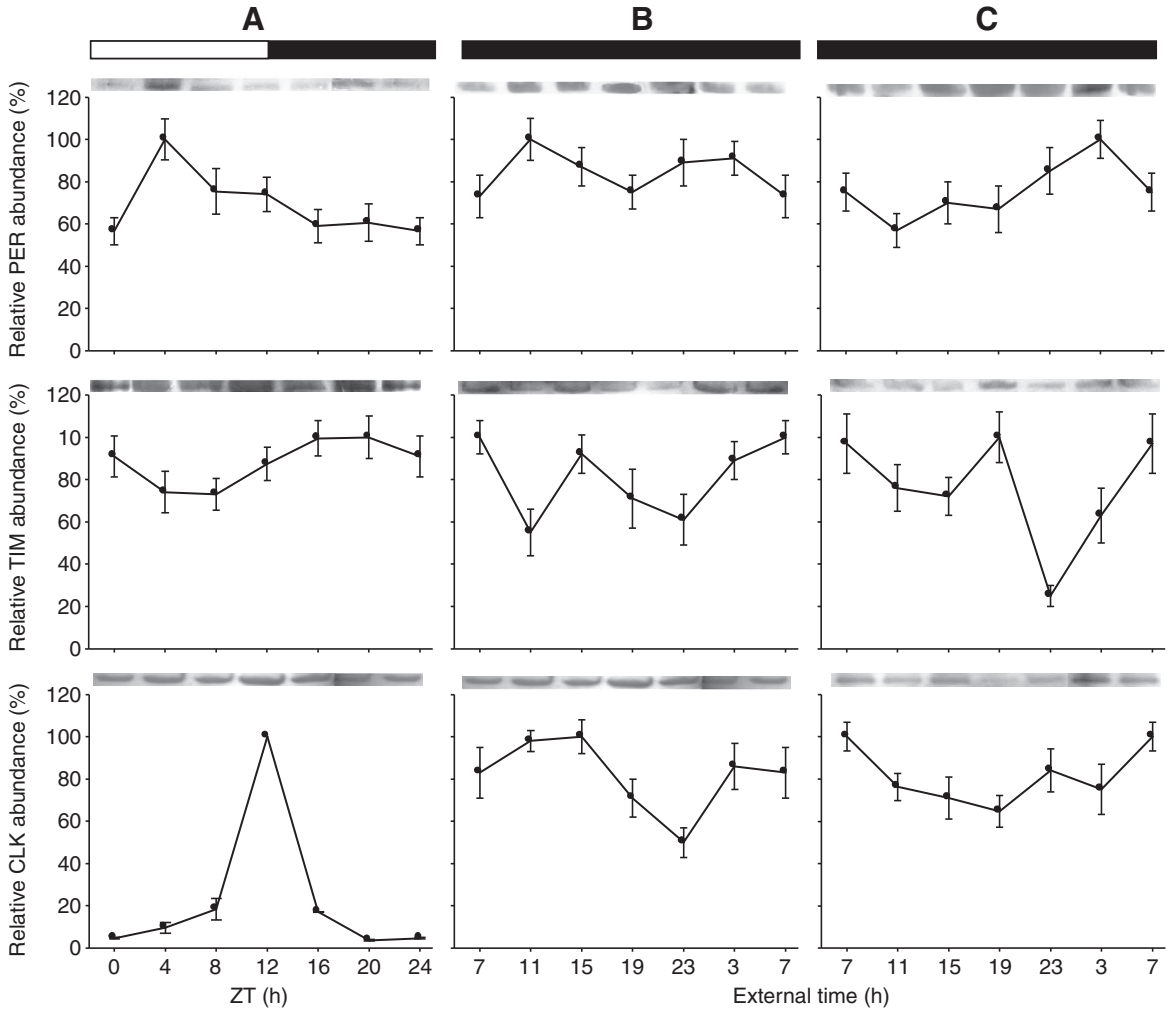

Fig. 7. Chronograms illustrating daily and circadian rhythms of PER, TIM and CLK abundance in *P. clarkii* eyestalk. Bars at the top indicate the illumination conditions (open, light; filled, dark). Representative western blots are shown at the top of each panel. Each lane represents the time point of the sample collection. (A) 12 h:12 h light:dark conditions; (B) 24 h of continuous darkness (D:D). Note the unimodal PER and ClK circadian rhythms and the statistically significant bimodal TIM rhythm. (C) 72 h of D:D. PER, TIM and CLK oscillate, showing statistically significant circadian rhythms (see Table 2). The data for B and C were obtained from tissues of animals maintained in the dark for 24 and 72 h, respectively. Panel A shows data obtained from animals maintained in L:D conditions. Values are means ± s.e.m. (*N*=6).

have not been reported before. The overall distribution of these antigens suggests that these three circadian proteins interact with each other in the putative circadian oscillators of crayfish: retina, optic lobe and brain. This supports previous hypotheses about the distributed multi-oscillatory nature of the circadian system of crayfish (Aréchiga and Rodríguez-Sosa, 2002; Fanjul-Moles and Prieto-Sagredo, 2003).

It is now recognized that daily rhythms of behavior are controlled by a circuit of circadian pacemaker neurons (Tomioka and Matsumoto, 2010). Our results indicate that the neural cells located in the retina, optic ganglia lamina and medullas, as well as in the lateral protocerebrum and brain (Sandeman et al., 1992), express three clock proteins that are considered to be the pre- and post-transcriptional elements that form the molecular clock loops (Hardin, 2005). However, we only detected the necessary nuclear expression in some of these cells (Fig. 3B–D, Fig. 4A,C and Fig. 5E,G).

The presence of these clock proteins in the cytoplasm and/or nucleus of several retina, optic lobe and brain cells, depending on the ZT (Fig. 3B,C, Fig. 4A and Fig. 5E,G), as well as their colocalization, suggests interactions between positive and negative transcription factors and clock proteins similar to those that form the feedback loop of the canonical model proposed for different animals (Stanewsky, 2003; Vansteensel et al., 2008).

Although we only explored two times of day in the present study, the cellular colocalization of antigens suggests negative or positive interaction among these proteins at ZT 0 in the eyestalk and at ZT 12 in the brain. The consistent colocalization of these proteins in the eyestalk and retina, in the somata of cells distributed throughout all soma clusters of the four major neuropils of the optic lobe and the brain, and in clusters 6 and 10, is particularly interesting. Both 5-hydroxytryptamine (5-HT)-ir and 5-HT receptors have been reported in these locations (Sandeman et al., 1988; Spitzer et al., 2005). 5-HT has been proposed to be a modulator of circadian rhythms in crayfish (Castañón-Cervantes et al., 1999; Wildt et al., 2004). Other works from our lab have reported expression of another circadian protein, CRY, but its expression is restricted to cells in the lateral and median protocerebrum (Fanjul-Moles et al., 2004; Escamilla-Chimal and Fanjul-Moles, 2008).

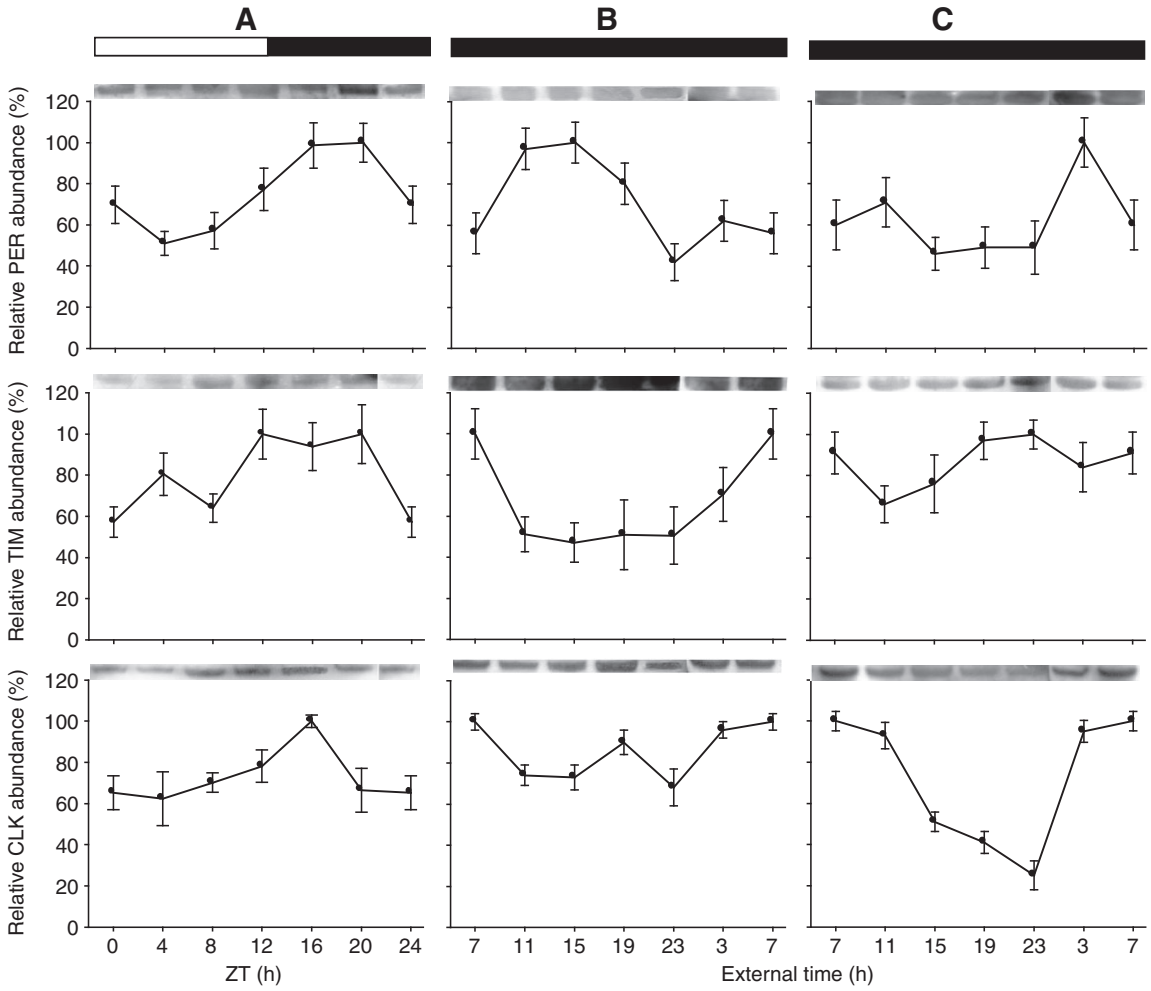

Fig. 8. Chronograms illustrating daily and circadian changes of PER, TIM and CLK abundance in *P. clarkii* brain. Bars at the top indicate the illumination conditions (open, light; filled, dark). Representative western blots are shown at the top of each panel. Each lane represents the time point of the sample collection. (A) 12 h:12 h light:dark (L:D) conditions. PER and CLK show statistically significant daily oscillations (PER $P<0.05$, $N=9$, CLK $P<0.05$, $N=9$). (B) 24 h of continuous darkness (D:D). PER and TIM revealed circadian oscillations; however, CLK presented a statistically significant bimodal rhythm. (C) 72 h of D:D. Note that the three proteins showed statistically significant circadian oscillations (PER $P<0.01$, TIM $P<0.05$, CLK $P<0.01$, $N=9$ for each point and antigen; see Table 2). Values are means ± s.e.m. ($N=6$).

Biochemical assessment

The biochemical assay demonstrated PER, TIM and CLK circadian functionality. Both in the eyestalk and in the brain, the protein levels underwent apparent daily and circadian rhythms, proven as statistically significant by the cosinor analysis (Table 2). However, in L:D, some features of the rhythm, particularly the phase, were different for each structure. Unexpectedly, eyestalk PER maximal abundance occurred at ZT 04.00, in the middle of day, whereas TIM and CLOCK peaked at ZT 20.00 and ZT 12.00, respectively. This is contrary to what has been previously reported for *Drosophila,* where the binding of PER and TIM with dCLK occurs at the end of the night (Meyer et al., 2006). Here we show that, after the maximal peak, crayfish PER relative abundance decreases but always maintains relatively high values (60% of maximal). In *Drosophila*, it has been reported that PER persists after TIM is, in part, eliminated by light (Shafer et al., 2002), binding to TIM later in the night to translocate into the nucleus, abrogating the binding of the CLK–CYC heterodimer to the PER promoter. A similar phenomenon may occur in crayfish, as our immunochemical results have revealed nuclear PER only at the end of the night at ZT 0 in eyestalk (Fig. 3B–D) and at the beginning of the night at ZT 12 in cluster 6 of protocerebral cells (Fig. 5E,G).

Daily oscillations of the abundance of brain PER and TIM cycle with a temporal pattern similar to those of *Drosophila*, peaking at night and decreasing in the morning. This suggests the reciprocal autoregulation of their own transcription, as has been proposed for *Drosophila* (Zeng et al., 1996). In contrast to dCLK, which peaks in abundance around dawn, after maximal dTIM and dPER oscillations, crayfish CLOCK peaks at night. This protein shows only one peak that coincides with PER and TIM maximal phases, suggesting that these proteins might bind to CLK, abrogating their own transcription. Yang et al. (Yang et al., 2006) have reported the presence of *clk* in the prawn *Macrobrachium rosenbergii* (mar-*clock*). Although these authors reported neither daily nor circadian oscillations of this gene, expression of mar-*clock* tended to increase at ZT 18. Although speculative, these findings and our results suggest that, in crustaceans, almost no phase lag between *CLK* mRNA and protein expression occurs, as has been proposed for dCLK (Glossop et al., 1999). In other aquatic organisms, the *CLK* mRNA cycle peaks during the night

at ZT 15 (Whitmore et al., 1998). Here, we show that, in crayfish brain, TIM, PER and CLOCK cycle with a maximal phase occurring at night. Immunochemical assessment revealed that PER-ir and CLOCK are present in the nucleus of different cells at night (Fig. 5B,E,G). This suggests that both proteins in crayfish are transcription modulators. Previous research from our laboratory has demonstrated the presence of another circadian protein, CRY, in the brain of crayfish, with the CRY cycle peaking at night (Fanjul-Moles et al., 2004). Hence, although some authors have recently demonstrated that CRY is linked to photoreception of the clock in crayfish (Sullivan et al., 2009), the possibility exists that, as with insects, CRY in crayfish functions pleiotropically in circadian rhythm generation.

LIST OF ABBREVIATIONS

AL	accessory lobe
AMPN	anterior median protocerebral neuropil
AnN	antennal neuropil
dCLK	Clock of *Drosophila*
dCRY	Cryptochrome of *Drosophila*
dCYC	cycle of *Drosophila*
D:D	continuous darkness
DE	deutocerebrum
dPdp	Par Domain Protein 1 of *Drosophila*
dPER	Period of *Drosophila*
dTIM	Timeless of *Drosophila*
EM	external medulla
GAPDH	glyceraldehyde-3-phosphate dehydrogenase
HB	hemillipsoid body
IGL	internal ganglion cell layer
IM	internal medulla
ir	immunoreactivity
L:D	light:dark conditions
LG	lamina ganglionaris
LPR	lateral protocerebrum
MPR	medial protocerebrum
OL	olfactory lobe
PGS	proximal glial sheath
PR	percentage of rhythmicity
PT	protocerebral tract
RPCH	red pigment concentrating hormone
TM	terminal medulla
TR	triticerebrum
v/v	volume/volume
w/v	weight/volume
XO-SGT	X-organ sinus gland tract
ZT	Zeitgeber time
τ	period

ACKNOWLEDGEMENTS

We thank Alejandro Martinez Mena for his support with Apotome microscopy and Guadalupe Sandoval González for her technical help. Financial support was provided by PAPITT no. IN207008. We appreciate the comments of the anonymous reviewers, which greatly improved the manuscript.

REFERENCES

Aréchiga, H. and Rodríguez-Sosa, L. (1998). Circadian clock function in isolated eyestalk tissue of crayfish. *Proc. R. Soc. Lond. B. Biol. Sci.* **265**, 1819-1823.

Aréchiga, H. and Rodriguez-Sosa, L. (2002). Distributed circadian rhythmicity in the crustacean nervous system. In *The Crustacean Nervous System* (ed. K. Wiese), pp. 113-122. Heidelberg: Springer-Verlag.

Barrera-Mera, B. and Block, G. D. (1990). Protocerebral circadian pacemakers in crayfish: evidence for mutually coupled pacemakers. *Brain Res.* **522**, 241-245.

Bradford, M. M. (1976). A rapid and sensitive method for the quantitation of microgram quantities of protein utilizing the principle of protein dye binding. *Anal. Biochem.* **248**, 25-32.

Castañón-Cervantes, O., Battelle, B. and Fanjul-Moles, M. L. (1999). Rhythmic changes in the serotonin content of the brain and eyestalk of crayfish during development. *J. Exp. Biol.* **202**, 2823-2830.

Darlington, T. K., Wager-Smith, K., Ceriani, M. F., Staknis, D., Gekakis, N., Steeves, T. D. L., Weitz, C. J., Takahashi, J. S. and Kay, S. A. (1998). Closing the circadian loop: CLOCK-induced transcription of its own inhibitors *per* and *tim*. *Science* **280**, 1599-1603.

DeCoursey, J. P. (1983). Biological timing. In *Behavior and Ecology. The Biology of Crustacea* (ed. E. D. Bliss, F. Vernberg and B. W. Vernberg) pp. 210-277. New York: Academic Press.

Dubruille, R. and Emery, P. (2008). A plastic clock: how circadian rhythms respond to environmental cues in *Drosophila*. *Mol. Neurobiol.* **38**, 129-145.

Escamilla-Chimal, E. G. and Fanjul-Moles, M. L. (2008). Daily and circadian expression of cryptochrome during the ontogeny of crayfish. *Comp. Biochem. Physiol.* **151A**, 461-470.

Fanjul-Moles, M. L. (2006). Biochemical and functional aspects of crustacean hyperglycemic hormone in decapod crustaceans: review and update. *Comp. Biochem. Physiol.* **142C**, 390-400.

Fanjul-Moles, M. L. and Prieto-Sagredo, J. (2003). The circadian system of crayfish: a developmental approach. *Microsc. Res. Tech.* **60**, 291-301.

Fanjul-Moles, M. L., Escamilla-Chimal, E. G., Gloria-Soria, A. and Hernández-Herrera, G. (2004). The crayfish *Procambarus clarkii* CRY shows daily and circadian variation. *J. Exp. Biol.* **207**, 1453-1460.

Glossop, N. R. J., Lyons, L. C. and Hardin, P. E. (1999). Interlocked feedback loops within the *Drosophila* circadian oscillator. *Science* **286**, 766-768.

Hafner, G. S. (1973). The neural organization of the lamina ganglionaris in the crayfish: a Golgi and EM study. *J. Comp. Neurol.* **152**, 255-280.

Hardin, P. E. (2005). The circadian timekeeping system of *Drosophila*. *Curr. Biol.* **15**, R714-R722.

Hardin, P. E. (2009). Molecular mechanisms of circadian timekeeping in *Drosophila*. *Sleep Biol. Rhythms* **7**, 235-242.

Laemmli, U. K. (1970). Cleavage of structural proteins during the assembly of the head of bacteriophage T4. *Nature* **227**, 680-685.

Larimer, M. J. L. and Smith, J. T. F. (1980). Circadian rhythm of retinal sensitivity in the crayfish: modulation by the cerebral and optic ganglia. *J. Comp. Physiol.* **136**, 313-326.

Menna-Barreto, L. A., Benedito-Silva, A., Marques, M., Andrade, M. and Louzada, F. (1993). Ultradian components of the sleep wake-cycle in babies. *Chronobiol. Int.* **10**, 103-108.

Meyer, P., Saez, L. and Young, M. W. (2006). PER-TIM interactions in living *Drosophila* cells: an interval timer for the circadian clock. *Science* **311**, 226-229.

Nassel, D. R. (1977). Types and arrangements of neurons in the crayfish optic lamina. *Cell Tissue Res.* **179**, 45-75.

Nelson, W., Tong, Y. L., Lee, J. K. and Halberg, F. (1979). Methods for cosinor-rhythmometry. *Chronobiol.* **6**, 305-323.

Page, T. L. and Larimer, J. L. (1975a). Neural control of circadian rhythmicity in the crayfish. I. The locomotor activity rhythm. *J. Comp. Physiol. A* **97**, 59-80.

Page, T. L. and Larimer, J. L. (1975b). Neural control of circadian rhythmicicty in the crayfish. II. The ERG amplitude rhythm. *J. Comp. Physiol.* **97**, 81-96.

Preciado, M., Tsutsumi, V. and Aréchiga, H. (1994). Ultrastructural features of neurosecretory cells in the external medulla of the crayfish eyestalk. *Gen. Comp. Endocrinol.* **95**, 432-442.

Sandeman, D. C., Sandeman, R. E. and Aitken, A. R. (1988). Atlas of serotonin-containing neurons in the optic lobes and brain of the crayfish, *Cherax destructor*. *J. Comp. Neurol.* **269**, 465-478.

Sandeman, D. C., Sandeman, R. E., Derby, C. and Schmidt, M. (1992). Morphology of the brain of crayfish, crabs and spiny lobsters: a common nomenclature for homologous structures. *Biol. Bull.* **183**, 304-326.

Shafer, O. T., Rosbash, M. and Truman, J. M. (2002). Sequential nuclear accumulation of the clock proteins period and timeless in the pacemaker neurons of *Drosophila melanogaster*. *J. Neurosci.* **22**(14), 5946-5954.

Spitzer, N., Antonsen, B. L., Donald, H. and Edwards, D. (2005). Immunocytochemical mapping and quantification of expression of a putative type 1 serotonin receptor in the crayfish nervous system. *J. Comp. Neurol.* **484**, 261-282.

Stanewsky, R. (2003). Genetic analysis of the circadian system in *Drosophila melanogaster* and mammals. *J. Neurobiol.* **54**, 111-114.

Sullivan, J. M., Genco, M. C., Marlow, E. D., Benton, J. L., Beltz, B. S. and Sandeman, D. C. (2009). Brain photoreceptor pathways contributing to circadian rhythmicity in crayfish. *Chronobiol. Int.* **26**, 1136-1168.

Tomioka, K. and Matsumoto, A. (2010). A comparative view of insect circadian clock systems. *Cell. Mol. Life Sci.* **67**, 1397-1406.

Vansteensel, M. J., Michel, S. and Meijer, J. H. (2008). Organization of cell and tissue circadian pacemakers: a comparison among species. *Brain Res. Rev.* **58**, 18-47.

Whitmore, D., Foulkes, N. S., Strähle, U. and Sassone-Corsi, P. (1998). Zebrafish Clock rhythmic expression reveals independent peripheral circadian oscillators. *Nat. Neurosci.* **1**, 701-707.

Wildt, M., Goergen, E. M., Benton, J. L., Sandeman, D. C. and Beltz, B. S. (2004). Regulation of serotonin levels by multiple light-entrainable endogenous rhythms. *J. Exp. Biol.* **207**, 3765-3774.

Yang, J. S., Dai, Z. M., Yang, F. and Yang, J. W. (2006). Molecular cloning of *Clock* cDNA from the prawn, *Macrobrachium rosenbergii*. *Brain Res.* **1067**, 13-24.

Zeng, H., Qian, Z., Myers, M. P. and Rosbash, M. (1996). A light-entrainment mechanism for the *Drosophila* circadian clock. *Nature* **380**, 129-135.